IJIRR

International Journal of Information Research and Review
Vol. 06, Issue, 03, pp.6190-6193, March, 2019

RESEARCH ARTICLE

THE EFFECT OF ELECTRON DENSITY INSTABILITIES ON DOSE CALCULATION

*,[1]Neeraj Verma and [2]Chetan Dhital

[1]Hind Institute of Medical Sciences, Barabanki, Safedabad, Utter Pradesh, India
[2]Department of Physics, College of Science and Mathematics, Kennesaw State University, Kennesaw, GA, USA

ARTICLE INFO

Article History:
Received 07th December, 2018
Received in revised form
08th January, 2019
Accepted 17th February, 2019
Published online 30th March, 2019

Keywords:

IVDT, Electron Density, Tomotherapy, IGRT, EBRT.

***Corresponding author:** Neeraj Verma

ABSTRACT

Treatment plans are based on an anatomical dataset of the tumor acquired during the preparation stage using a kVCT (kilovolt computed tomography) scanner. Anatomical reference changes will occur during the treatment course, in some cases requiring a new treatment plan to deliver the prescribed dose. With the introduction of 3D volumetric on-board imaging devices, it became feasible to use the produced images for dose recalculation. However, the use of these on-board imaging devices in clinical routine for the calculation of dose depends on the stability of the images. In this study the validation of tomotherapy MVCT (megavolt computed tomography) produced images, for the purpose of dose recalculation by the Planned Adaptive software, has been performed. To determine the validity of MVCT images for dose calculation, a treatment plan was created based on kVCT-acquired images of a solid water phantom. During a period of 5 months, MVCT images of the phantom have been acquired and were used by the planned adaptive software to recalculate the initial kVCT-based dose on the MVCT images. The impact of the adjusted IVDTs (image value to density table) has been explored just as the impact of picture procurement with or without going before airscan. Yield changes or potentially insecurities of the imaging bar result in MV images of various quality yielding diverse outcomes when utilized for portion estimation. It was demonstrated that the yield of the imaging bar isn't steady, prompting contrasts of almost 3% between the first kV-based portion and the recalculated MV-based portion, for strong water as it were. MVCT images can be utilized for portion estimation purposes remembering that the outcome is at risk to variances. The procurement of an IVDT together with the MVCT image set, that will be utilized for portion is suggested.

INTRODUCTION

Tomotherapy HiArt II (Tomotherapy Inc., Madison, WI, USA) is an intensity- modulated (IMRT) and image-guided (IGRT) radiotherapy modality. Usually megavolt (MV) images are acquired and registered with the planning kilovolt (kV) images to ensure correct patient positioning according to the kV-planning setup (Yadav *et al*., 2010). Along with its use for image guidance, MV images can also be used to verify the delivered dose based on the patient anatomy of the day. At the point when anatomical changes are available, a portion recalculation can be performed to evaluate the degree of the portion deviation contrasted with the first arranging portion. In principle, this data could be consolidated in versatile radiotherapy systems to adjust for dosimetric errors brought about by anatomical changes amid treatment (Barateau *et al*., 2015, Woodford *et al*., 2007). In order to use CT images (kV or MV) for dose calculation, a conversion table of image gray value to densities has to be created. The conversion table is also called the 'image value-to-density table' (IVDT) and is recorded using designated tissue characterization phantoms on the imaging modalities (Yadav *et al*., 2010). For a dose calculation algorithm that takes tissue in homogeneities into account, such as superposition convolution used by tomotherapy. It is very useful to establish the IVDT accurately (Cozzi *et al*., 1998). As a rule, treatment plan portions are determined dependent on kVCT-gained images. The quality of the kVCT images is observed and continued at the radiology division utilizing built up rules and quality confirmation protocols. Nonetheless, so as to adjust medicines, understanding images should be gained over the span of treatment to evaluate the anatomical circumstance and portion appropriation. The motivation behind this work is to test the consistency of the tomotherapy MV imaging abilities so as to figure portion, in view of the obtained images (Yadav *et al*., 2010). At the rationale of composing, no reasonable rules or quality affirmation conventions exist to keep up a steady imaging yield for the online-obtained MV images.

MATERIALS AND METHODS

Tomotherapy MVCT imaging: Tomotherapy MV images are obtained utilizing a xenon gas-filled imaging locator exhibit, mounted on the ring gantry inverse to the radiation source (Keller *et al*., 2002).

The radiation source has a nominal energy of 5.7 MV in treatment mode and will be detuned for the imaging mode which results in better imaging characteristics (Meeks *et al* 2005). Figure 1 shows Gammex phantom setup on machine bore. Three available imaging modes can be chosen on the administrator station: coarse, ordinary and fine. These imaging modes are classified by a pitch factor of, individually, 3, 2 and 1, and forwards recreated images with a transverse cut separately at, 6, 4 and 2 mm respectively (Jiang *et al* 2007, Song *et al* 2012, Chapman *et al*., 2015). Machine sinogram is shown in Figure 2. For this examination images were procured utilizing the ordinary imaging mode. No institutionalized imaging shaft qualities or bar profiles are accessible.

Figure 1. GMMA phantom with multiple density plugs on treatment modality bore

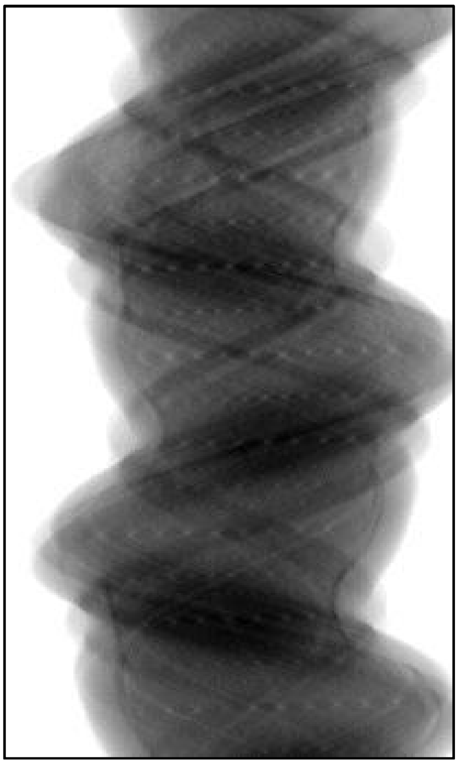

Figure 2. MV sonogram with overlapping blur due to target degradation over time

The Creation of an IVDT: For the computation of retained portion in the patient, in view of CT information, thickness data is expected to measure the shaft weakening along its way. An adjusted connection between the dark estimations of the CT images (kV or MV) and the thickness data is ordinarily settled utilizing a tissue portrayal phantom. The phantom used in this study is the Gammex Tomo Phant (Gammex, Middleton, WI, USA) with 12 calibrated density rods ranging from 0.3 g cm^{-3} (Lung, LN-300) to 1.82 g cm^{-3}. The density rods were evenly distributed over the phantom holes and the same arrangement was used for all the acquisitions and such a pluggable phantom helps in adjusting the anatomical variations (Yadav *et al*., 2010). To begin with, the tissue portrayal phantom was imaged with kVCT (Siemens SOMATOM Emotion 16, Erlangen, Germany) with the imaging protocol utilized in clinical practice (Yu *et al*., 2015). Second, the mean dim estimation of the individual thickness plugs was gotten from the procured images. The IVDT can be finished across the mean dimensional estimation of the individual plugs with the real arranged physical densities. The IVDTs are sustained to the arranging station, and the fitting table, contingent upon the utilized imaging protocol, must be chosen when beginning a treatment plan.

Reference with a solid water phantom: Analysis was started from scratch, the Gammex TomoPhant was imaged on the kVCT scanner (Siemens SOMATOM Emotion16, Erlangen, Germany) with solid water and tissue characterization rods to create, respectively, a new kVCT-based treatment plan using solid water and the most up-to-date IVDT. The treatment plan consisted of a 132-cc target volume in the middle of the phantom, and no organs at risk were defined. A field width of 30 mm and a pitch of 0.254 was used to optimize the treatment plan with a prescribed dose of 20 Gy on a normal calculation grid. The prescribed dose was fractionated into ten fractions resulting in a beam-on time of 146 sec per fraction. Once approved, the treatment plan can be accessed from the workstation station to scan MVCT images. Total phantom image and its position with focus on isocenter of the machine to avoid image set overlap are used (Jursinic *et al*., 2010). The phantom with the tissue characterization rods was imaged using the normal imaging mode on tomotherapy to create the IVDTs (Yadav *et al*., 2010). Images were exported to OsiriX for the extraction of the ROI data of the density rods. IVDTs were created and transferred onto the tomotherapy planning station for the dose calculation in PA module. The formation of a check plan with portion determined on MVCT images begins with the determination of the ideal IVDT, MV scan set and treatment plan sinogram. Inflexible image enrollment between the kV and MV images must be performed to guarantee that the treatment is conveyed by the kV treatment plan (Yadav *et al*., 2010). After the enlistment, the image position is spared, and the portion estimation can be performed. Langen *et al* have appeared, in the wake of going for a thorough method to make IVDTs, a phenomenal understanding (under 0.35%) can be achieved when contrasting MVCT determined portion and kVCT-determined portion, utilizing unbending phantoms.

Scan variations: The yield of the machine is checked utilizing portion chambers, yet no portion rate control servo is available in the framework to tune the yield progressively. In this way, the portion chamber yield is kept inside specs by applying portion check levels for the treatment bar.

The Greetings Workmanship portion checking will end a treatment methodology if the pillar yield is outside a ±4% window for 12 seconds or outside a ±40% window for 2 seconds. Plot of phantom density with radiation source is shown in Figure 3 and normalized dose is shown in Figure 4. This does exclude yield varieties because of gantry revolution. The movement of the shaft yield because of gantry turn is added to the portion checking window up to ±2% of the normal pillar yield. For the imaging beam, however, only an upper reference is set to make sure that the imaging dose to the patient will be limited. When applying the same levels for the imaging beam as for the treatment beam, the system will terminate the imaging procedure regularly because the lower dose checking window level will be reached. This was an indication that the imaging beam output was not stable within a range of ±4%. Variations to the dose-chamber counts during imaging were recorded for each imaging procedure during several months (Yadav *et al*., 2010).

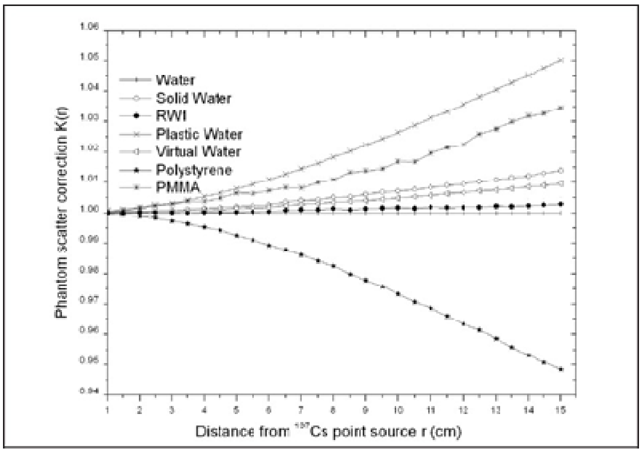

Figure 3. Phantom material density with respect to scatter from radiation source

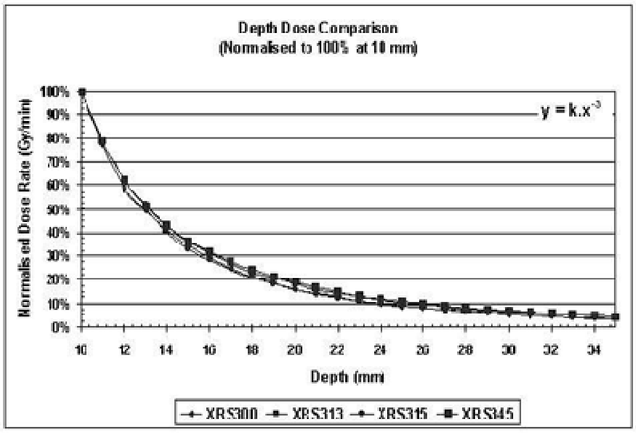

Figure 4. Normalized dose distribution for variation in scan distance from target source

RESULTS

Reference with a solid water phantom: IVDT, observed originally, was tested for MV images acquired during 3 weeks at random intervals after performing an airscan. All dose readings were obtained from the DVH, and the mean dose (D50) was tracked. Results show that a maximum discrepancy between the kV-planned dose and the verification doses of 2% using solid waterdensity only. MV verification doses were much less than the planned dose, meaning that the phantom material has been synchronized by the IVDT into denser material than the original. The difference increases overtime, basically due to deterioration in electron density (Yadav *et al*., 2010). System component wear, for example target degradation, seems unlikely because of the short time span of the subsequent image acquisitions and no component replacements or specific machine instabilities occurred during this short period of acquisitions (Yadav *et al*., 2010). When using the same $IVDT_{(A)}$ for images acquired after a few months, discrepancies become even more substantial. Differences of nearly 4% between the planned dose and verification dose was observed when using an IVDT recorded several months before the MV image acquisition due to target degradation. Based on previous results, it seems that the drift increases after a few months, but images acquired 1 week later show a small drift. The dose difference between the planned dose and verification dose has now been reduced from nearly 3% to 1%. This event indicates that the system is liable to 'certain' fluctuations and that this influences the MV images that are used for dose calculation (Yadav *et al*., 2010). At the time of the acquisition of image set, a new $IVDT_{(B)}$ was established as well. Subsequently, the dose of image set B was recalculated using the new $IVDT_{(B)}$ and the older $IVDT_{(A)}$ recorded during first acquisition a few months prior. Dose penumbera can be seen in Figure 5. Comparison of both IVDTs shows that the CT values for solid water are increased on the new $IVDT_{(B)}$ compared to the old $IVDT_{(A)}$. The same CT values will result in a lower density for dose calculation when using the new IVDT, yielding to a higher dose on the target volume. The difference between the planned dose and verification dose decreases to approximately 2% opposed to the 4% difference when using the prior $IVDT_{(A)}$.

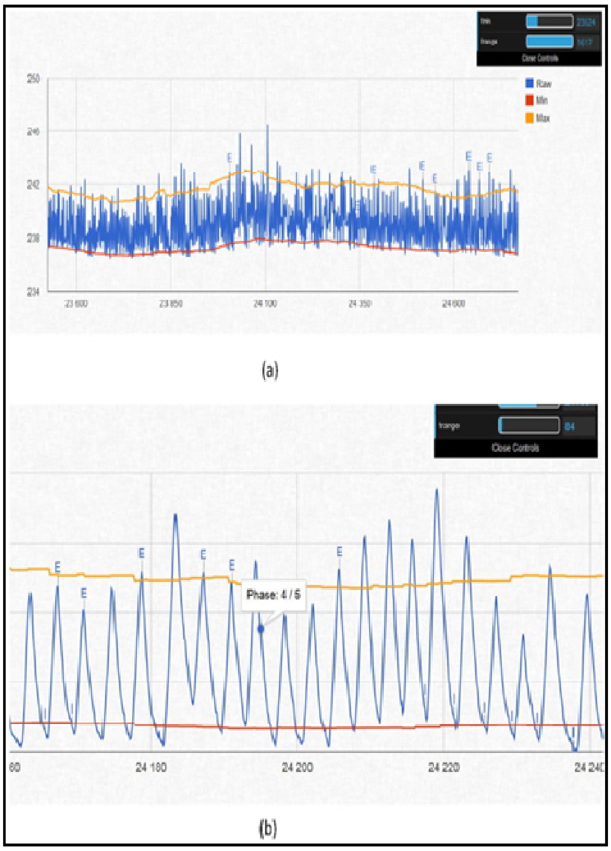

Figure 5. Radiation dose penumbra for phase cycles with outliners beyond min and max ranges

Scan Variations: To analyze the icon beam output variations for 3 days, we fetched the detector file from the system after imaging of each patient. The detector file records the imaging detector signals and dose chamber counts, during the image acquisition, at a frequency of 72 Hz. An in-house developed Matlab script was written to extract the dose chamber data from the detector file (dose chamber 1, closest to the linac). In total 41 patients were imaged during 2 days with an average imaging time of 173 seconds with a minimum and maximum imaging time of, respectively, 114 seconds and 313 seconds. The results of the reference test with a solidness water supply phantom show that the irradiation calculation is liable to certain fluctuation probably caused by the outturn of the imaging electron beam. The recorded dose chamber rotational variation during the acquisitions varied between 6% and 8%, while the average dose-chamber count varied up to 12% between acquisitions.

DISCUSSION AND CONCLUSION

As per the existing literature it is possible to recompute dose with a precision that is similar to that of computed dose using kVCT images (Langen *et al*., 2005). When using solid water phantom only, disagreement of at least 1% were found in our study when recalculating dose based on MV image sets using updated IVDT. Same IVDT when used for separate scan sets acquired for 05 months period, larger variant was observed. There was no vogue (up or down) of the magnitude of discrepancies which implicated that the tomography scheme is liable to short -full term fluctuation (Yartsev *et al*., 2007). Form narrow perspective, the imaging shaft of beam outturn for 2 days showed that imaging output fluctuation of 12% occurred, but the main cause of imaging beam output fluctuations remains target degradation (Yadav *et al*., 2010). Reduced machine output can have several causes: target degradation, magnetron aging, impedance mismatch, AFC tuning, etc. Staton *et al*. (2009) have shown that, on a long term, a decrease in beam energy can occur near the end of the target lifetime due to target degradation. As the radiation and imaging source is identical, it can be expected that target degradation will also have an influence on the imaging beam output and energy. At the end, more information is needed about the imaging beam adjustments, detuning of the linac for imaging and the influence of ambient parameters on the imaging detector. The establishment of designated quality assurance protocols should be initiated. The stability of the system, in terms of tomography turnout is susceptible to fluctuations and will affect the dosage calculation (Yadav *et al*., 2010).

Unstable imaging beam output will influence both the conception of IVDTs and the CT values in the acquired scans. When icon beam attenuation parameters are going to be used for dose recalculation, an IVDT acquired together with the image set is needed. This implies that the tissue characterization phantom has to be scan after performing an airs can and prior to the accomplishment of the image set that is to be used for dose calculation. Treatment adaptation in clinical praxis where daily persona is acquired to reminder or alter the dose delivery will become a comprehensive process this way. Stability of HU is an important factor considered in the treatment plan verification and accurate delivery in IGRT. This should be verified periodically with reference dose to the phantom and to validate image guidance scan variations should be measured.

REFERENCES

Barateau, Anaïs, Christopher Garlopeau, Audrey Cugny, Bénédicte Henriques De Figueiredo, Charles Dupin, Jérôme Caron and Mikaël Antoine, 2015. "Dose calculation accuracy of different image value to density tables for cone-beam CT planning in head & neck and pelvic localizations." *Physica Medica*, 31, 146-151.

Chapman, David, Shaun Smith, Rob Barnett, Glenn Bauman and Slav Yartsev, 2014. "Optimization of tomotherapy treatment planning for patients with bilateral hip prostheses." *Radiation Oncology,* 9, no. 1: 43.

Cozzi, Luca, Antonella Fogliata, Francesca Buffa and Sabine Bieri, 1998. "Dosimetric impact of computed tomography calibration on a commercial treatment planning system for external radiation therapy." *Radiotherapy and oncology,* 48, no. 3: 335-338.

Jiang, Hongyu, Joao Seco and Harald Paganetti, 2007. "Effects of Hounsfield number conversion on CT based proton Monte Carlo dose calculations." *Medical physics,* 34, no. 4: 1439-1449.

Jursinic, Paul A., Renu Sharma, and Jim Reuter. "MapCHECK used for rotational IMRT measurements: step-and-shoot, TomoTherapy, RapidArc." *Medical physics*, 37, no. 6Part1: 2837-2846.

Keller, Harry, Marvin Glass, Ralf Hinderer, K. Ruchala, Robert Jeraj, Olivera, G. and Rock Mackie, T. 2002. "Monte Carlo study of a highly efficient gas ionization detector for megavoltage imaging and image-guided radiotherapy." *Medical physics*, 29, no. 2: 165-175.

Langen, K. M., Meeks, S. L., Poole, D. O., Wagner, T. H., Willoughby, T. R., Kupelian, P. A., Ruchala, K. J., Haimerl, J. and Olivera, G. H. 2005. "The use of megavoltage CT (MVCT) images for dose recomputations." *Physics in Medicine and Biology,* 50, no. 18: 4259.

Meeks, Sanford L., Joseph F. Harmon, Katja M. Langen, Twyla R. Willoughby, Thomas H. Wagner, and Patrick, A. 2005. Kupelian. "Performance characterization of megavoltage computed tomography imaging on a helical tomotherapy unit." *Medical physics*, 32, no. 8: 2673-2681.

Song, Ju-Young and Sung-Ja Ahn, 2012. "Effect of image value-to-density table (IVDT) on the accuracy of delivery quality assurance (DQA) process in helical tomotherapy." *Medical Dosimetry*, 37, no. 3: 265-270.

Staton, Robert J., Katja M. Langen, Patrick A. Kupelian, and Sanford, L. 2009. Meeks. "Dosimetric effects of rotational output variation and x-ray target degradation on helical tomotherapy plans." *Medical physics,* 36, no. 7: 2881-2888.

Woodford, Curtis, Slav Yartsev, A. Rashid Dar, Glenn Bauman, and Jake Van Dyk, 2007. "Adaptive radiotherapy planning on decreasing gross tumor volumes as seen on megavoltage computed tomography images." International *Journal of Radiation Oncology* Biology* Physics,* 69, no. 4: 1316-1322.

Yadav, Poonam, Ranjini Tolakanahalli, Yi Rong, and Bhudatt R. Paliwal, 2010. "The effect and stability of MVCT images on adaptive TomoTherapy." *Journal of applied clinical medical physics*, 11, no. 4: 4-14.

Yartsev, S., Kron, T. and Van Dyk, J. 2007. "Tomotherapy as a tool in image-guided radiation therapy (IGRT): current clinical experience and outcomes." *Biomedical Imaging and Intervention Journal* 3, no. 1.

Yu, Jialu, Nicholas Hardcastle, Kyoungkeun Jeong, Edward T. Bender, Mark A. Ritter and Wolfgang, A. 2015. Tomé. "On voxel-by-voxel accumulated dose for prostate radiation therapy using deformable image registration." *Technology in cancer research and treatment,* 14, no. 1: 37-47.

****